Lodz University of Technology

Scientific Lectures 2024

# POWER GENERATION THROUGH VIBRATION-BASED ENERGY HARVESTERS

## a) Hybrid piezo-electromagnetic energy harvester
## b) Electromagnetic energy harvesters' array

**Rajarathinam Murugesan**

ADVISOR

**Prof. Jan Awrejcewicz**

**Department of Automation, Biomechanics and Mechatronics**

# Outline

- Introduction
- Literature Surveys
- Motivation and Objectives
- Investigation of hybrid harvester
- Demonstration of hybrid power application
- Investigation of an array of electromagnetic energy harvester
- Conclusion

# Introduction
# and
# Literature Survey

# Energy Harvesting

What is energy harvesting?

Extracting electrical energy from ambient resources which otherwise gets wasted.

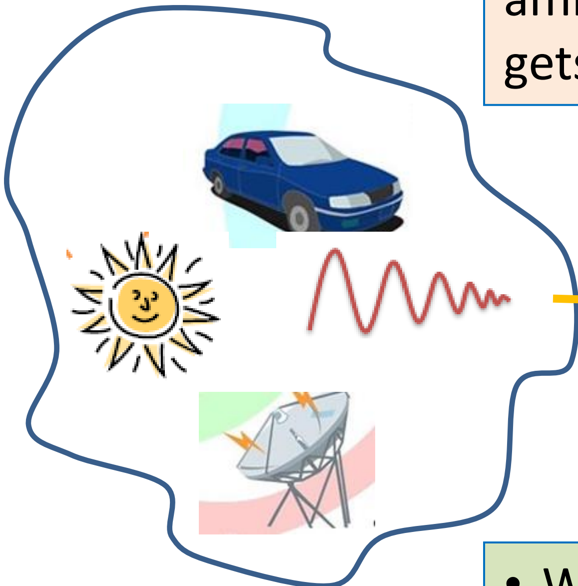

Ambient Energy

Harvester → Energy Storage

Transduction techniques

Capacitors

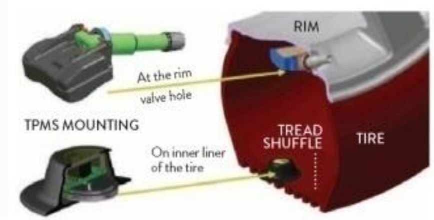


Sensors


Actuators

Low power devices

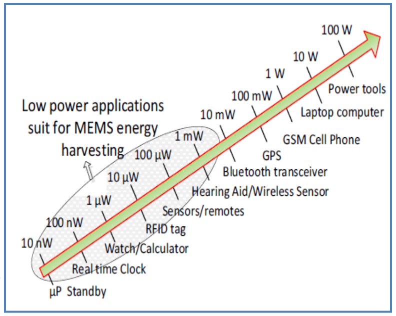


- Wireless applications.
- Condition monitoring: Bridge, Building, Traffic data, Health etc.,
- Major role: Smart homes, Smart buildings and Smart cities

micro-energy cell (MEC) product overview *Tech. Rep*

# Applications of energy harvesting

Wireless Sensor Networks (WSNs)

Environmental Monitoring

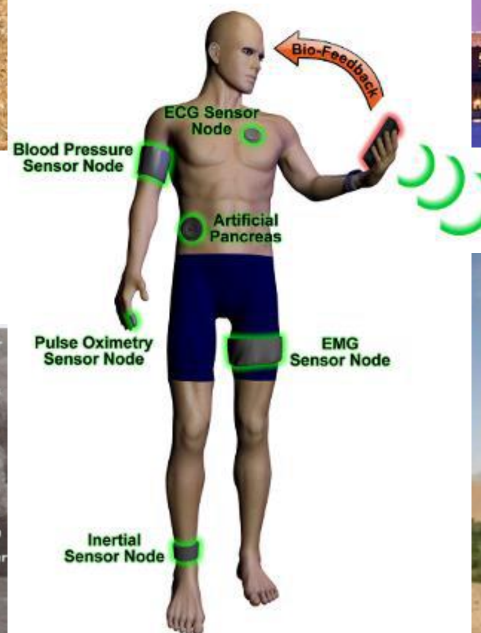


Medical remote sensing

Structural Monitoring

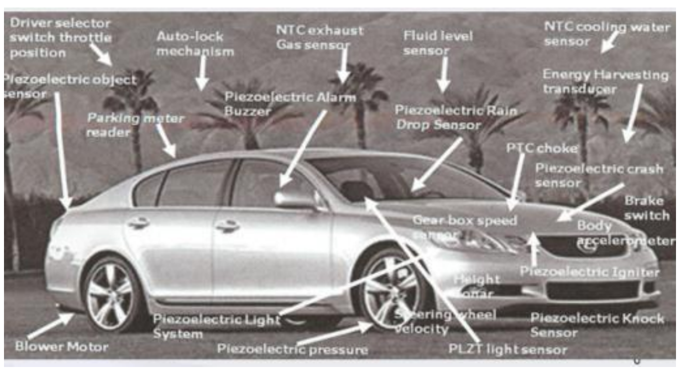


Automobile applications

Military applications

Almost 90% of WSNs applications cannot be enabled without Energy Harvesting technologies that allow self-powering features- F Cottone

# Vibration Energy Harvesters - Transduction Techniques

Electromagnetic: Any change in the magnetic field of a solenoid will induce an emf in the solenoid.

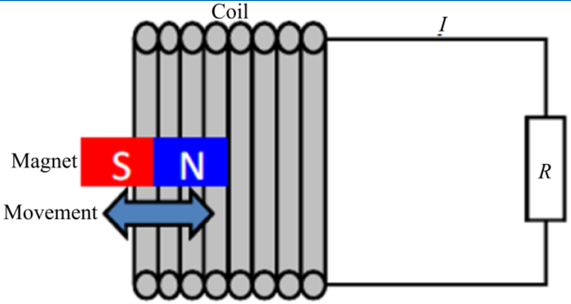


Magnetostrictive: Generates power because of change in magnetization due to applied stress.

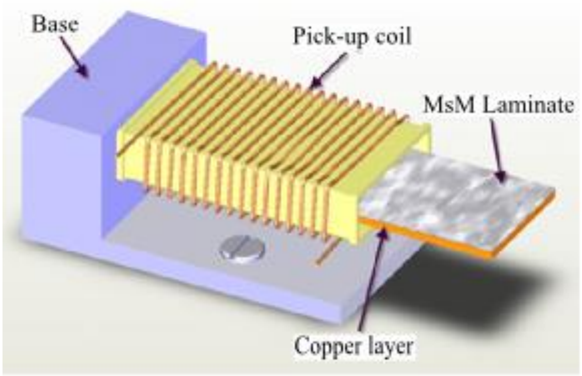


Why Vibration?: Commonly available in structural and industrial environments.

Electrostatic: Generates power when the transducer moves against an electrical field.

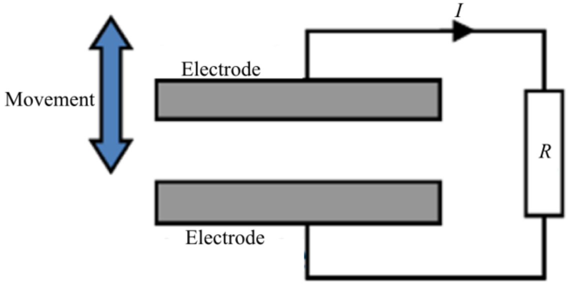


Piezoelectric: Generates power when mechanical stress is applied to the piezoelectric elements through external vibrations.

Boisseau et al.,2012

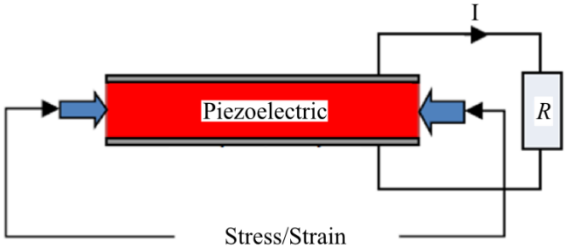

# Literature Survey

- Piezoelectric EH: High frequency, High voltage, Low current

- Electromagnetic EH: Low frequency, Low voltage, High current

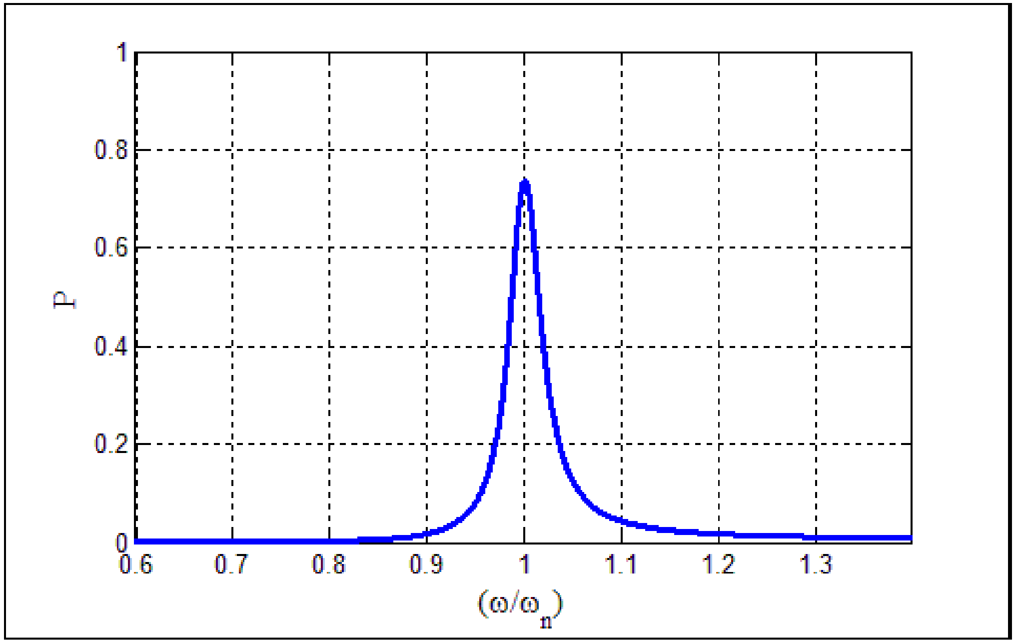


**Need of Hybrid Energy harvesting** (Tadesse *et al., 2009,* Khaligh *et al., 2010)*

**Why Broadband Energy harvesting?**

- Standalone linear harvester: Harvested power reduces drastically as the excitation frequency moves away from the resonant frequency.
- Ambient vibrations are random in nature; thus, these harvesters perform poorly under such excitations.

# Broadband energy harvesting

Increasing the operating bandwidth so that fairly large power output is obtained over a range of frequencies.

| Multi-frequency technique | Resonance tuning technique | Nonlinear harvesting technique |
| --- | --- | --- |

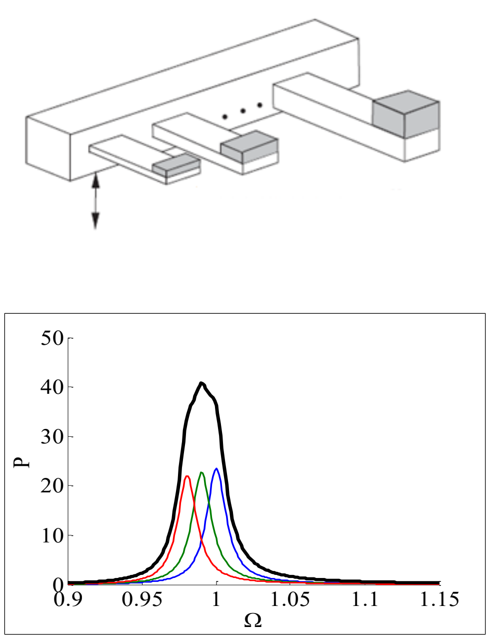


S.M. Shahruz (2008)

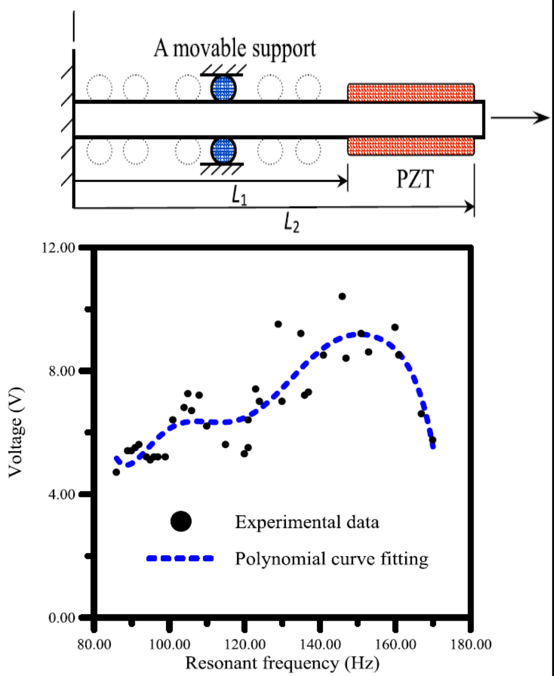


Huang and Lin, 2012

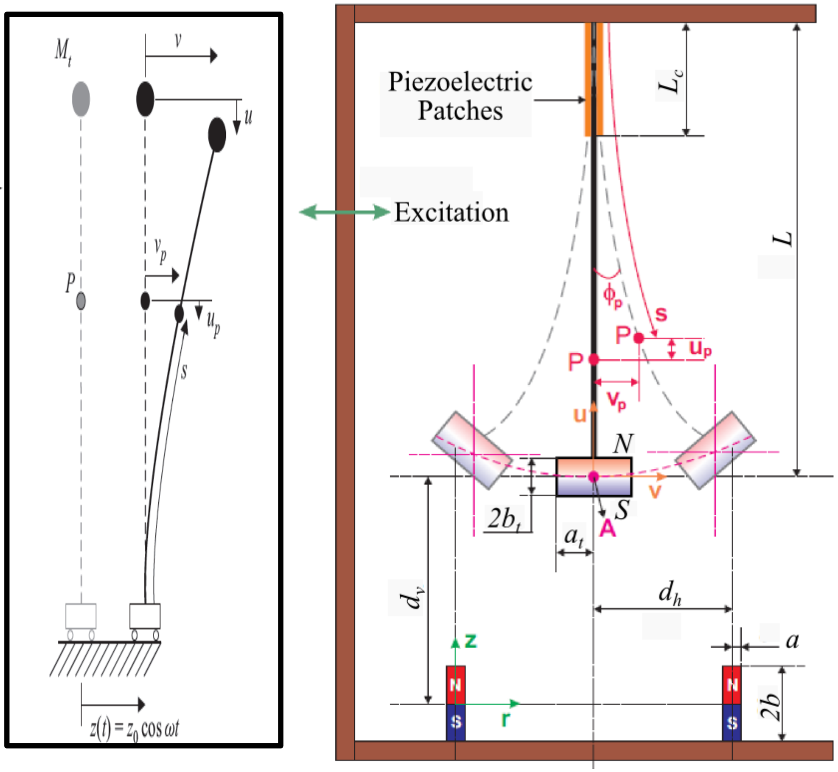


Friswell et al., 2012, Kumar et al., 2015

# Motivation and Objectives

Motivation :

- To scavenge a reasonable amount of power over a broad frequency range using:

(i) Hybrid transduction mechanism

(ii) Electromagnetic energy harvesters' array.

Objectives:

- Analysis of the hybrid energy harvester under harmonic and random excitations and comparing with the standalones.
- Verification of the results through experiments.
- Application of the generated power for wireless temperature and acceleration sensors.
- Investigation of an array of electromagnetic energy harvesters.

# I.Investigation of hybrid harvester under harmonic excitation

# Proposed Hybrid Piezo-Electromagnetic Energy Harvester

Harvesting energy using both piezoelectric and electromagnetic techniques in a single device.

## Harvester Model

First mode assumption

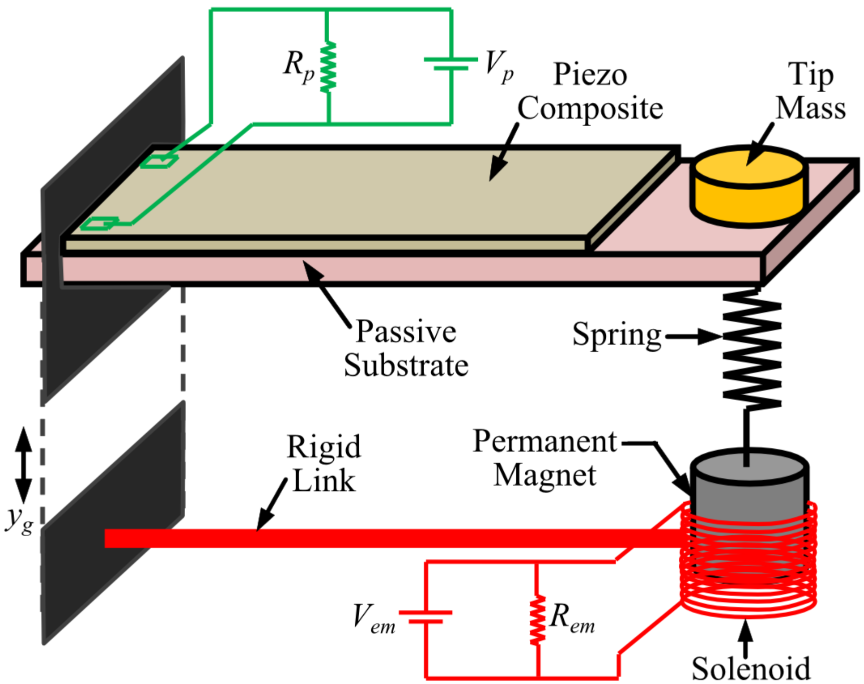


Physical Model

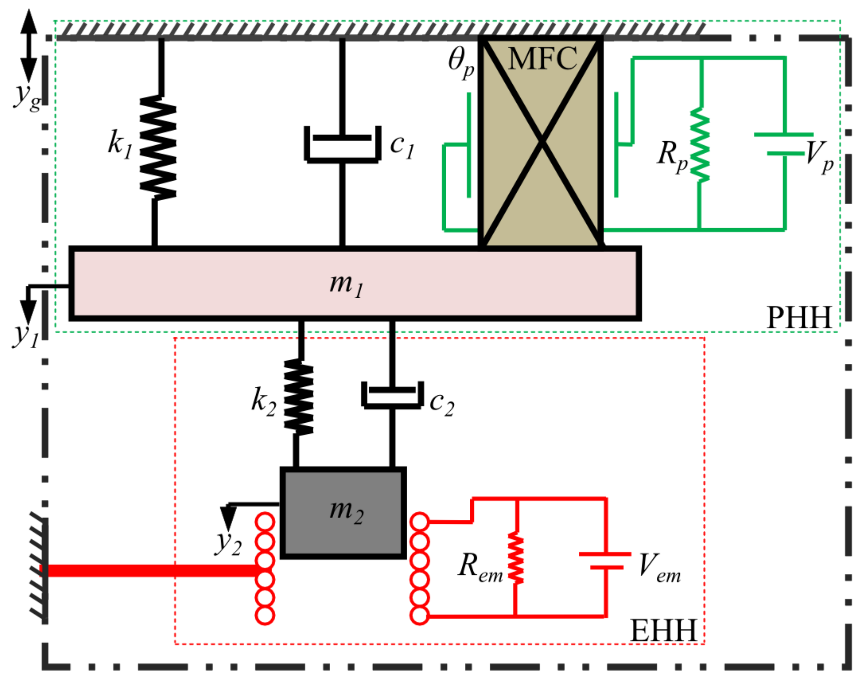


Equivalent Lumped Mass Model

# Mathematical Model-Harmonic analysis

Piezo-electro-magneto-mechanical model of the hybrid harvester is derived using Newton's second law of motion, piezoelectric constitutive law and Faraday's law of induction,

$$m_1\ddot{y}_{1r}(t)+c_1\dot{y}_{1r}(t)-c_2[\dot{y}_{2r}(t)-\dot{y}_{1r}(t)]+k_1y_{1r}(t)-k_2[y_{2r}(t)-y_{1r}(t)]+\theta_pV_p(t)=-\lambda m_1\ddot{y}_g(t)$$

$$m_2\ddot{y}_{2r}(t)+c_2[\dot{y}_{2r}(t)-\dot{y}_{1r}(t)]+k_2[y_{2r}(t)-y_{1r}(t)]=-m_2\ddot{y}_g(t)$$

$$-\theta_py_{1r}(t)+C_p\dot{V}_p(t)+\frac{V_p(t)}{\lambda R_p}=0$$

$$V_{em}(t)+\theta_{em}\dot{y}_{2r}(t)=0$$

Normalizing the equations w. r. t resonant frequency of the primary system,

$$[-\Omega^2+2\zeta_1 i\Omega+2\mu\beta\zeta_2 i\Omega+\mu\beta^2+1]Y_{1r}-[2\mu\beta\zeta_2 i\Omega+\mu\beta^2]Y_{2r}+\left[\frac{\theta_p}{k_1}\right]V_p=\lambda\Omega^2Y_g$$

$$-[2\beta\zeta_2 i\Omega+\beta^2]Y_{1r}+[-\Omega^2+2\beta\zeta_2 i\Omega+\beta^2]Y_{2r}=\Omega^2Y_g$$

$$-\left[\frac{\theta_p}{C_p}\alpha i\Omega\right]Y_{1r}+[i\alpha\Omega+1]V_p=0$$

$$V_{em}=-\theta_{em}\omega_1 i\Omega Y_{2r}$$

$$\left\{\begin{array}{l}\Omega=\dfrac{\omega}{\omega_1};\alpha=\lambda\omega_1C_pR_p\\ \beta=\dfrac{\omega_2}{\omega_1};\mu=\dfrac{m_2}{m_1};\kappa^2=\dfrac{\theta_p{}^2}{k_1C_p}\end{array}\right.$$

Power output,

$$\mathrm{P_{PHH}}=\frac{|V_p/\sqrt{2}|^2}{R_p};\qquad \mathrm{P_{EHH}}=\left|\frac{V_{em}/\sqrt{2}}{R_{em}+Rc}\right|^2R_{em}$$

Total Power $\mathrm{P_{HH}}=\mathrm{P_{PHH}}+\mathrm{P_{EHH}}$

# Experimental setup

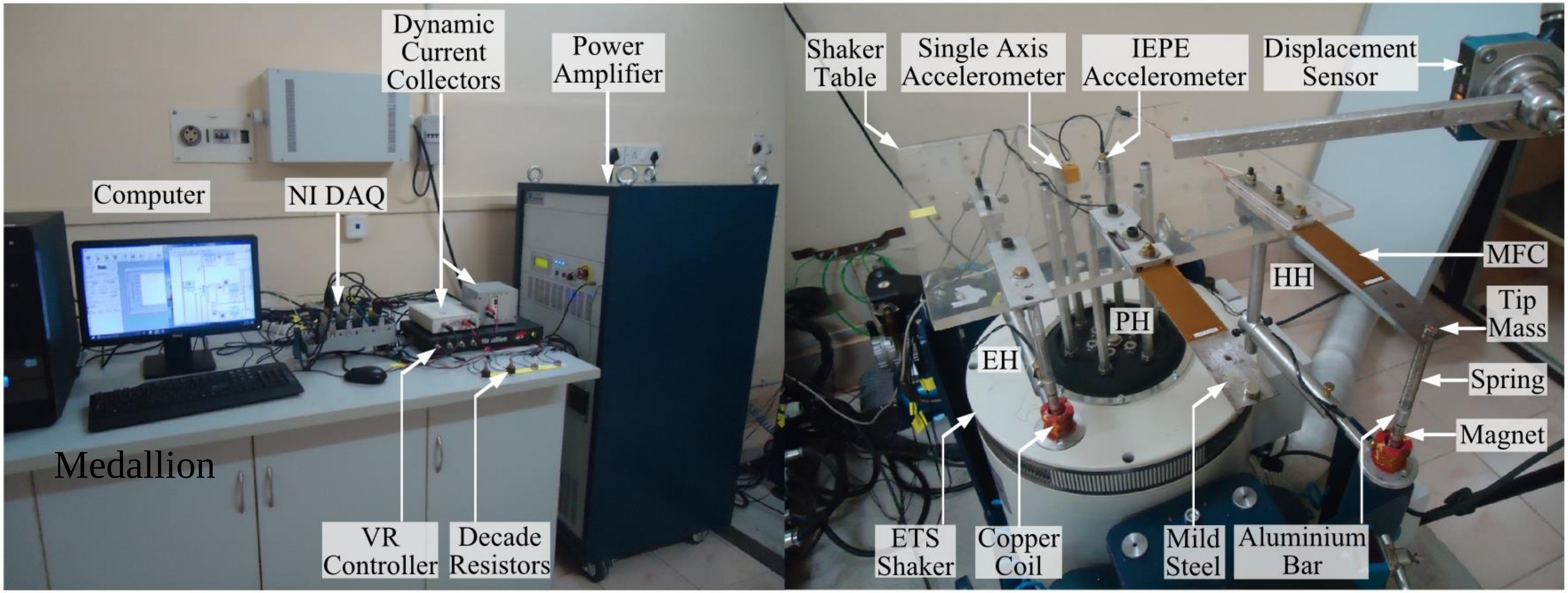


Fig: Photograph

Table: Parameters and their values

| Parameter | Value | Parameter | Value | Parameter | Value | Parameter | Value |
|---|---|---|---|---|---|---|---|
| $L$ | 160 mm | $\rho$ | 7800 kg/m³ | $C_p$ | 177.07 nF | $B_m$ | 1.1 T |
| $b$ | 32 mm | $t_p$ | 0.3 mm | $R_p$ | 50 kΩ | $R_{em}$ | 60 Ω |
| $t_b$ | 0.4 mm | $C^E$ | 15.857 Gpa | $m_t$ | 13.19 gm | $\zeta_1$ | 0.0238 |
| $E$ | 210 Gpa | $d_{31}$ | 170 pC/N | $m_m$ | 17.61 gm | $\zeta_2$ | 0.0044 |

Harmonic analysis

- Frequency sweep
  1-20Hz (Re 0.05Hz)
- Resistance sweep
  PE:10-200kΩ, EM10-200Ω
- Base excitation
  1mm

# Results: Harmonic analysis: contd…

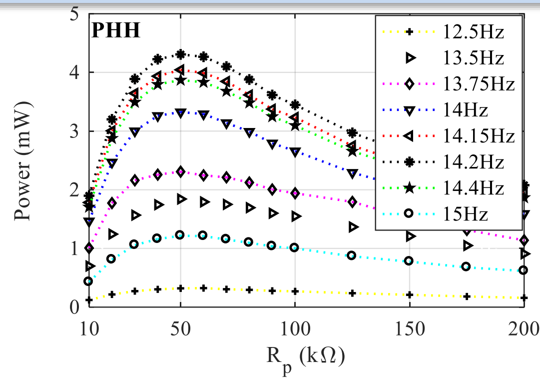


(a) Hybrid PE power with $R_p$

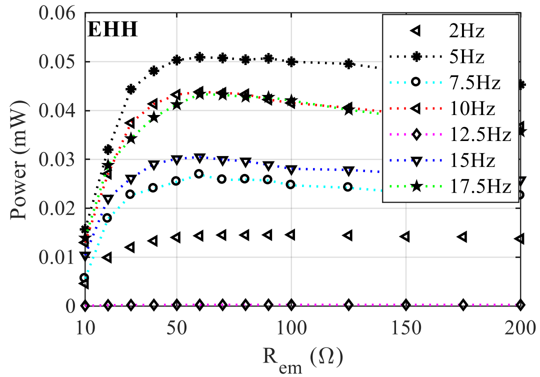


(b) Hybrid EM power with $R_{em}$

Figs : Variation of power with different set of load resistance

Optimal load resistance: $R_p$=50 KΩ; $R_{em}$=60 Ω

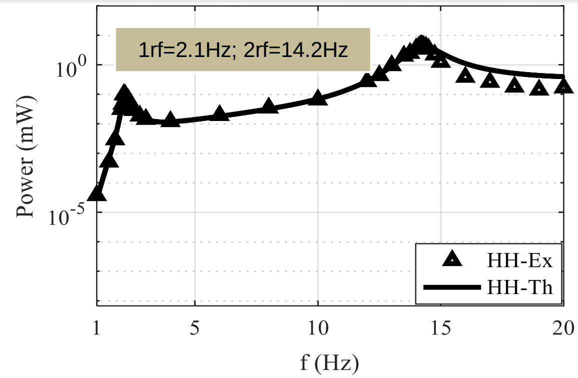


(a) HH power-in test and in simulation

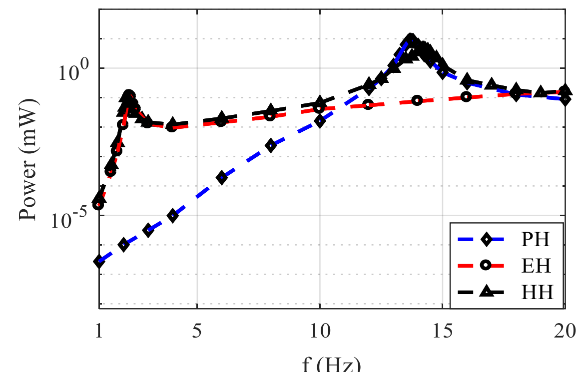


(b) Comparisons of experimentally obtained PH, EH and HH powers

Figs : Comparisons of Power outputs

The power harvested by the hybrid harvester exceeds the power obtained by standalone alternatives over a large region between the two resonating frequencies. This makes the hybrid harvester generate broadband power which is unachievable for standalone devices.

# Results: Harmonic analysis: Parametric study

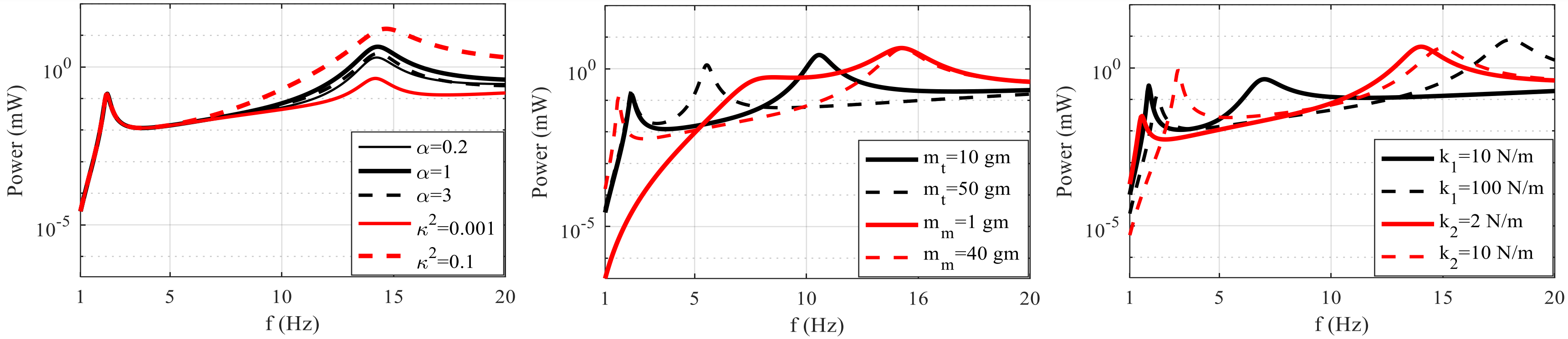


Figs: Power curves in hybrid energy harvester with different parameter values.

Table: Response of the hybrid harvester with respect to increase in parameters value

| Parameter | First Resonating Frequency | | | Second Resonating Frequency | | | Total Band Width |
|---|---|---|---|---|---|---|---|
| | Band Width | Power | $f_1$ Shift | Band Width | Power | $f_2$ Shift | |
| α | No change | No change | No change | Increase | Max at α = 1 | Slightly right | Slightly increase |
| $\kappa^2$ | Slightly decrease | Slightly decrease | No change | Increase | Increase | Right | Increase |
| $m_t$ | Slightly increase | Slightly increase | No change | Decrease | Decrease | Left | Decrease |
| $m_m$ | Decrease | Decrease | Left | No change | Decrease | Left | Increase |
| $k_1$ | No significant | Slightly decrease | Slightly right | Increase | Increase | Right | Increase |
| $k_2$ | Slightly decrease | Increase | Right | No change | No change | Right | Slightly decrease |

# Investigation of hybrid harvester under random excitation

# Mathematical Model-Random analysis

EOM:

$$m_1\ddot{y}_{1r}(t)+c_1\dot{y}_{1r}(t)-c_2[\dot{y}_{2r}(t)-\dot{y}_{1r}(t)]+k_1y_{1r}(t)-k_2[y_{2r}(t)-y_{1r}(t)]+\theta_pV_p(t)=-\lambda m_1\ddot{y}_g(t)$$

$$m_2\ddot{y}_{2r}(t)+c_2[\dot{y}_{2r}(t)-\dot{y}_{1r}(t)]+k_2[y_{2r}(t)-y_{1r}(t)]=-m_2\ddot{y}_g(t)$$

Gaussian

$$-\theta_py_{1r}(t)+C_p\dot{V}_p(t)+\frac{V_p(t)}{\lambda R_p}=0$$

$$V_{em}(t)+\theta_{em}\dot{y}_{2r}(t)=0$$

Power output:

$$P_{PHH}(t)=\frac{(V_p)^2}{R_p};\,P_{EHH}(t)=\left[\frac{-\theta_{em}V_{em}}{[R_{em}+R_c]}\right]^2R_{em}$$

Total Power

$$P_{HH}(t)=P_{PHH}(t)+P_{EHH}(t)$$

Based on the acceleration random input, the expected value arrived at

$$E[u_j(t)^2]=\frac{E\left[u_j(t)\right]^2}{c}=\int_{-\infty}^{\infty}\frac{1}{\left[\Delta(i\Omega)\right]^2}\frac{\left[H_j(\Omega)\right]^2}{\Omega^4}d\Omega$$

$$u_j(t)\longrightarrow y_{1r}(t),y_{2r}(t),V_p(t),V_{em}(t)$$

Solved by using classical Cramer's formula

Expected Power:

$$E[P_{HH}]=\frac{E[V_p{}^2]}{R_p}+\frac{E[V_{em}{}^2]}{[R_{em}+Rc]^2}R_{em}$$

Random analysis

| | | |
|---|---|---|
| Base excitation: Band limited GWN | $F_{band}$:2-5 Hz, 5-10 Hz, 10-15 Hz, 15-20 Hz, 2-10 Hz, 10-20 Hz, 2-20 Hz, 3.8-12.6Hz | Each frequency band- $\sigma_{acc}$ is different |

# Results: Random analysis

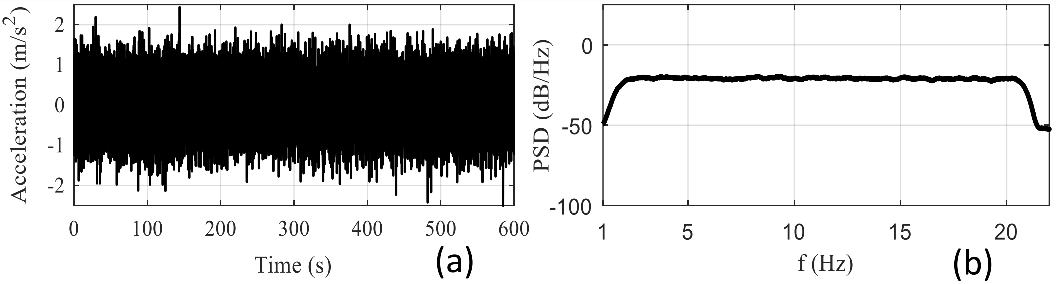


Band 2- 20 Hz
μ≈0
$\sigma_{acc}$= 0.5232

Figs: Input excitation at the harvester base (a) recorded time histories (b) PSD

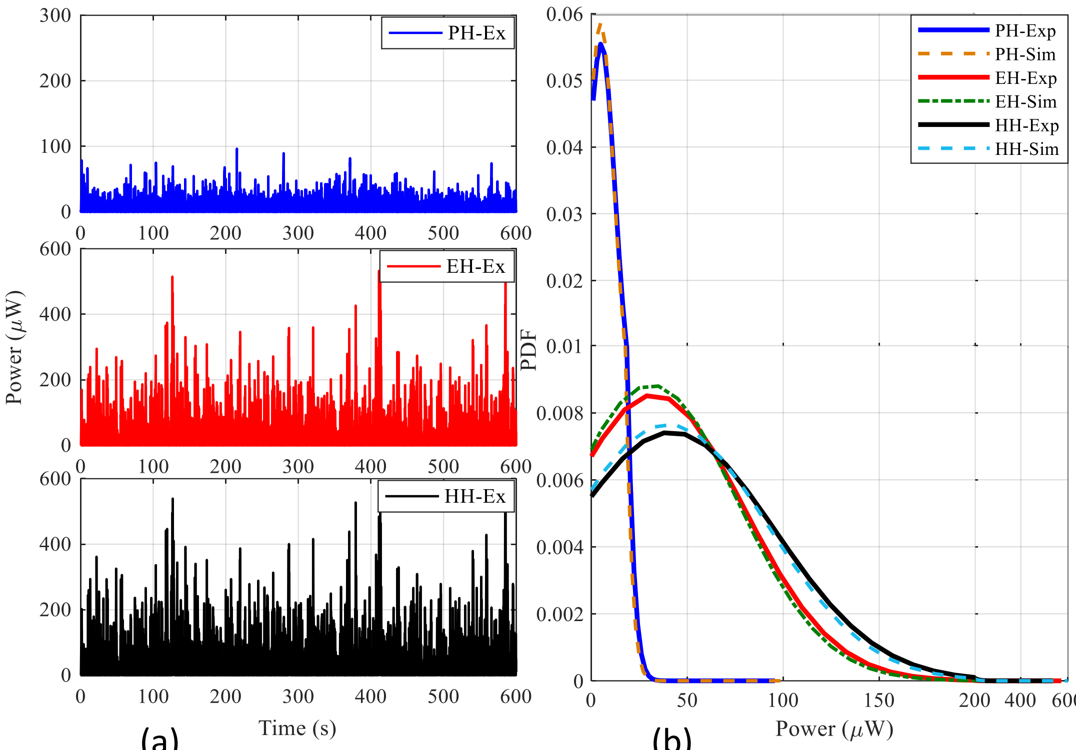


Simulation Power
PH=4.83 μW
EH=31.17 μW
HH=39.81 μW

Experimental Power
PH=5.11 μW
EH=32.63 μW
HH=41.80 μW

Figs : Comparisons of (a) power output obtained in tests (Ex: Experimental) for random base motion, corresponding (b) PDF with comparison of simulations (Th:Simulations)

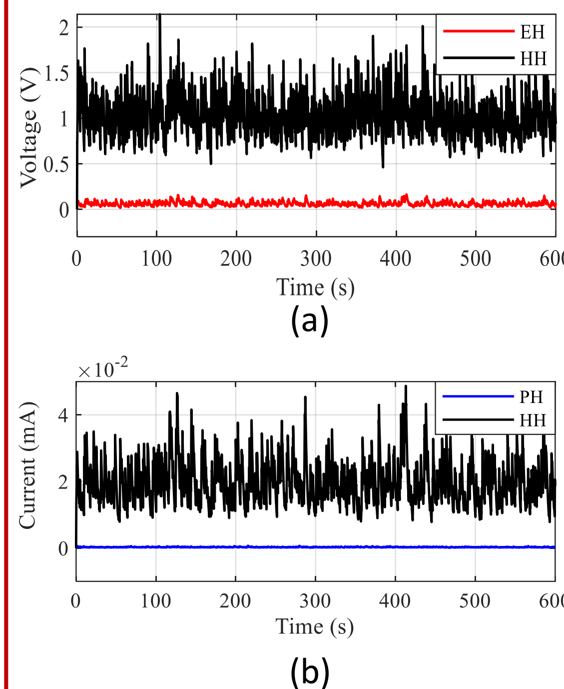


Figs : a) Comparisons of EH and HH voltages. (b) Comparisons of PH and HH currents.

# Results: Random analysis: contd…

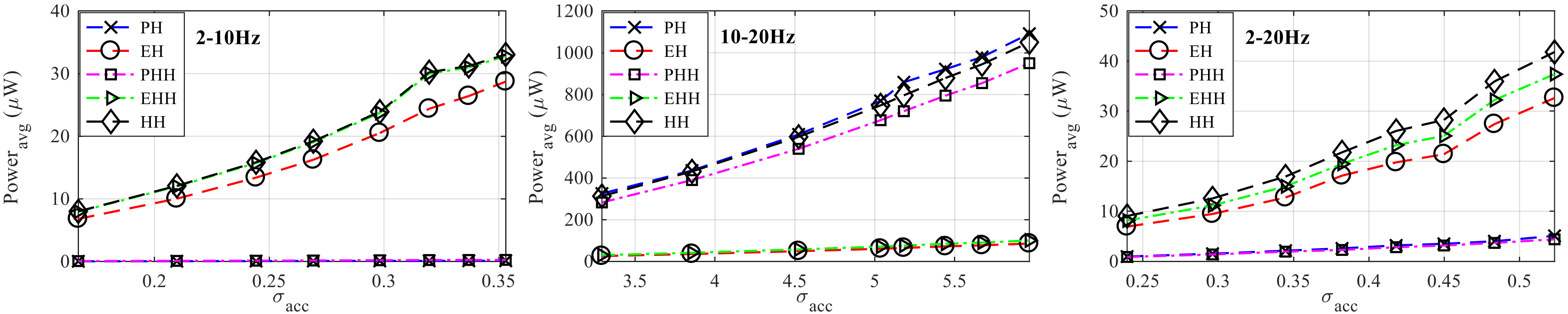


Fig: Average power versus standard deviation of input acceleration for different frequency bands

Table : Average power comparison of harvesters

| Frequency Range | PH | EH | HH | | | PH+EH | HH |
|---|---|---|---|---|---|---|---|
| | | | PHH | EHH | Total | | |
| 2-5 Hz | I | III | II | IV | V | Low | High |
| 5-10 Hz | I | III | II | IV | V | Low | High |
| 10-15 Hz | V | I | III | II | IV | High | Low |
| 15-20 Hz | III | II | IV | I | V | Low | High |
| 2-10 Hz | I | III | II | IV | V | Low | High |
| 10-20 Hz | V | I | III | II | IV | High | Low |
| 2-20 Hz | II | III | I | IV | V | Low | High |
| 3.8-12.6 Hz | II | III | I | IV | V | Low | High |

- In the frequency bands between 2–10Hz, the EM harvesters perform better compared to PE harvesters.
- In the frequency bands between 10–20Hz, the PE harvester perform better than EM harvesters.
- HH performs better between the first and second resonating frequencies (3.8–12.6Hz) and in the wide bandwidth (2–20Hz).

# Results: Random analysis: Parametric study

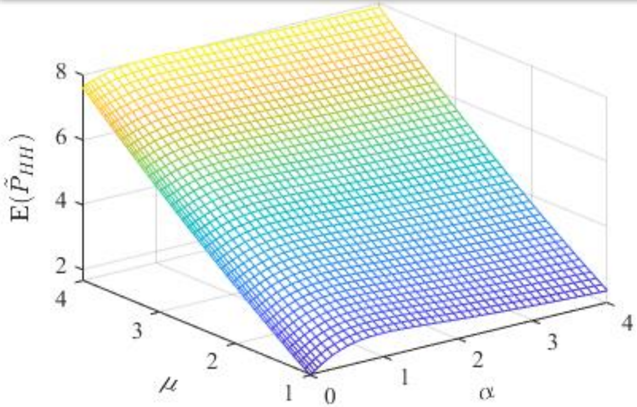


(a)

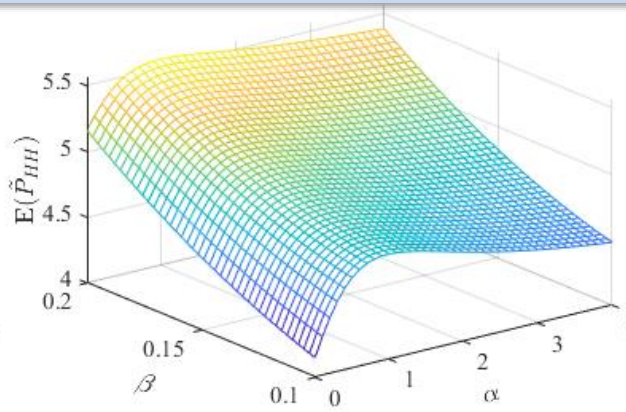


(b)

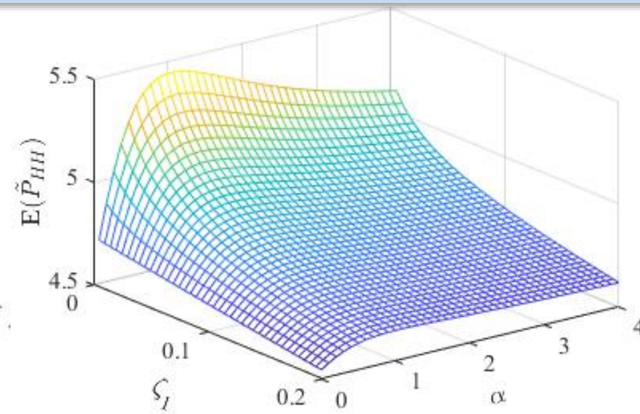


(c)

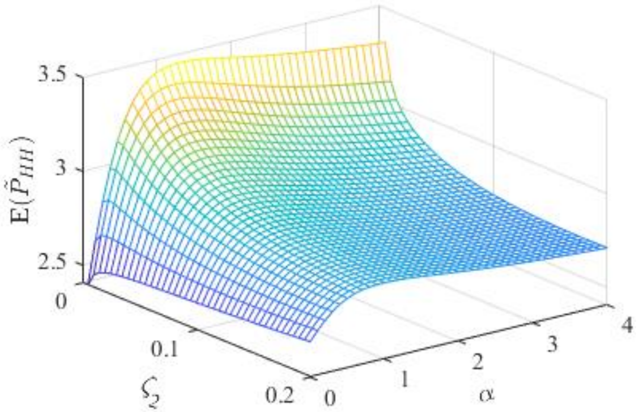


(d)

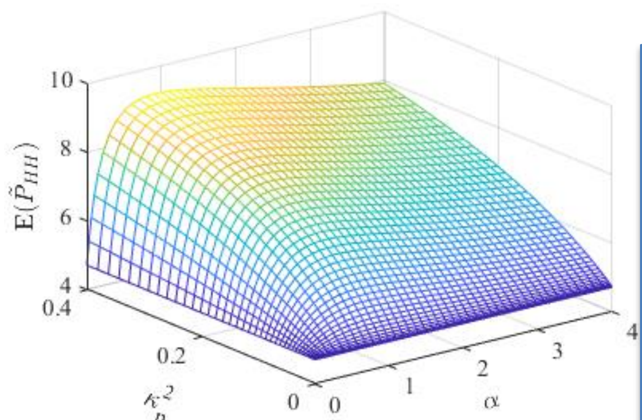


(e)

- Power increases with increasing the mass ratio, frequency ratio and electromechanical coupling coeff.
- Power decreases with increasing damping ratio of the PHH, EHH.
- Power increases with α till a maximum is reached. $\alpha_{max} = 1$.

Figs: Variation of HH normalized mean power as a function of non-dimensional time constant, α and (a) mass ratio, $\mu$ (b) frequency ratio, $\beta$ (c) damping ratio of the PHH, $\zeta_1$ (d) damping ratio of the EHH, $\zeta_2$ (e) non-dimensional electromechanical coupling coefficient .[Parameters other than the one being studied are considered as $\mu$=2.6318, $\beta$=0.1643, $\zeta1$=0.0238, $\zeta 2s$=0.0613, $\zeta em$=0.0569, $\kappa_p^2$=0.016.]

# Demonstration of hybrid power application

# Demonstration :I

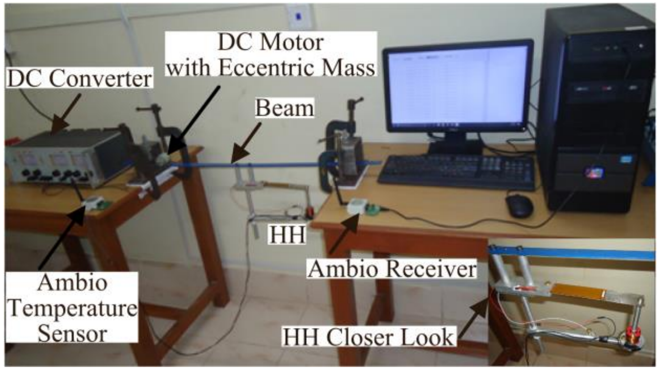


(a) Wireless temperature sensor powered from HH.

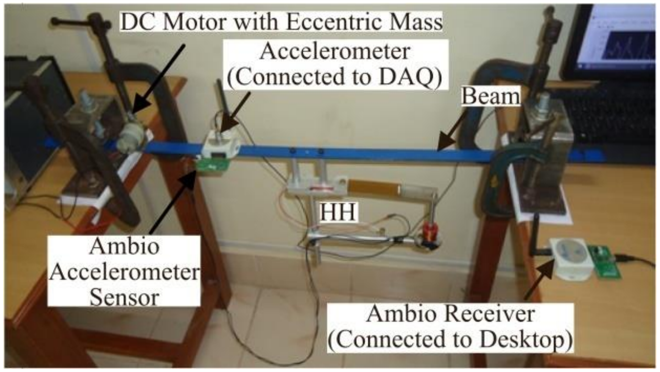


(b) Wireless accelerometer sensor powered from HH.

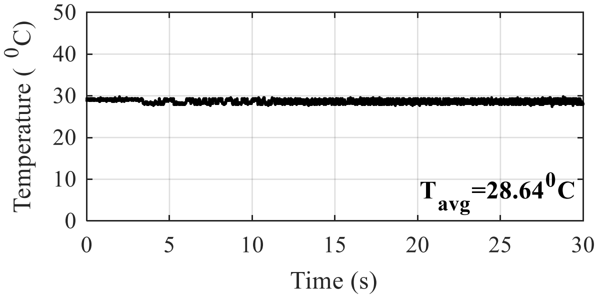


(c) Recorded temperature

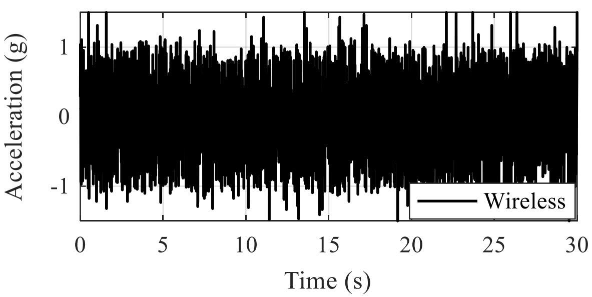


(d) Recorded acceleration signal from wireless accelerometer.

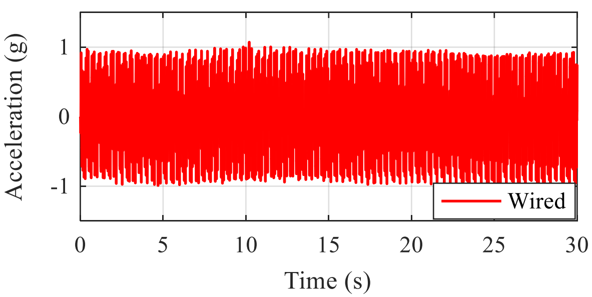


(e) Recorded acceleration signal from wired accelerometer.

Figs. Experimental demonstration of wireless sensors on a beam powered through hybrid harvester
(a) wireless temperature sensor, (b) wireless accelerometer sensor; recorded (c) temperature, (d) and (e) accelerations.

The wireless accelerometer is powered using HH for realizing the self-energized structural health monitoring

# Demonstration: II&III

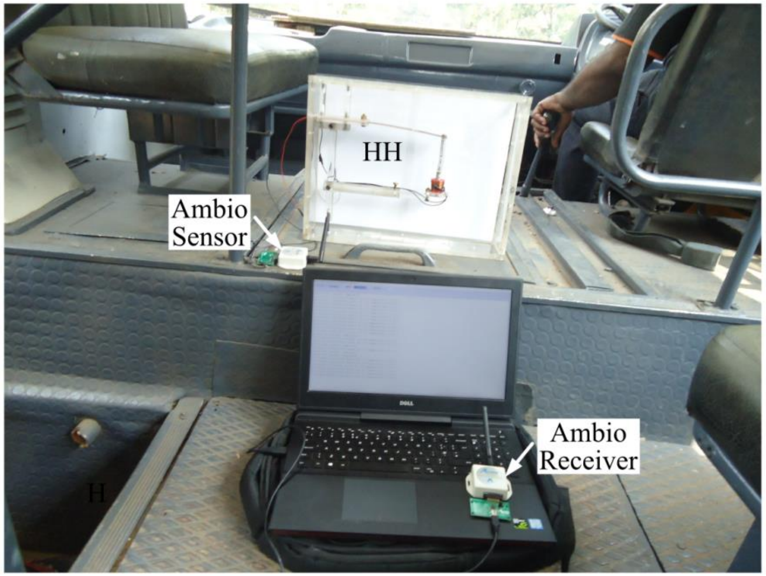


(a)

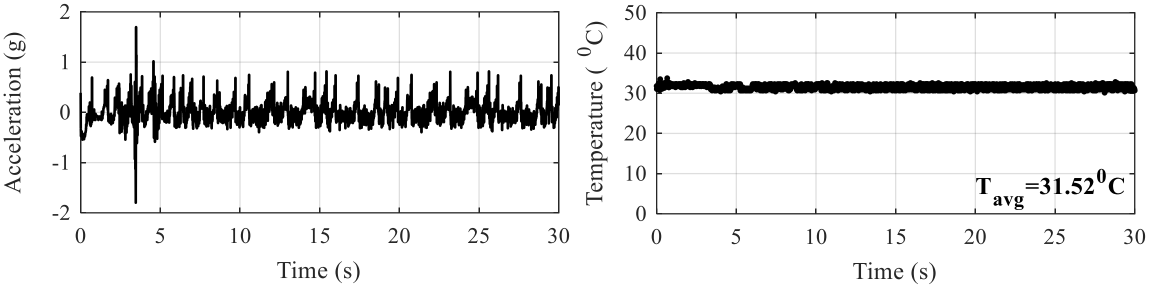


(b) (c)

Figs: Experimental demonstration of wireless sensors on a bus powered through hybrid harvester (a) setup of wireless sensor, (b) recorded acceleration, (c) recorded temperature.

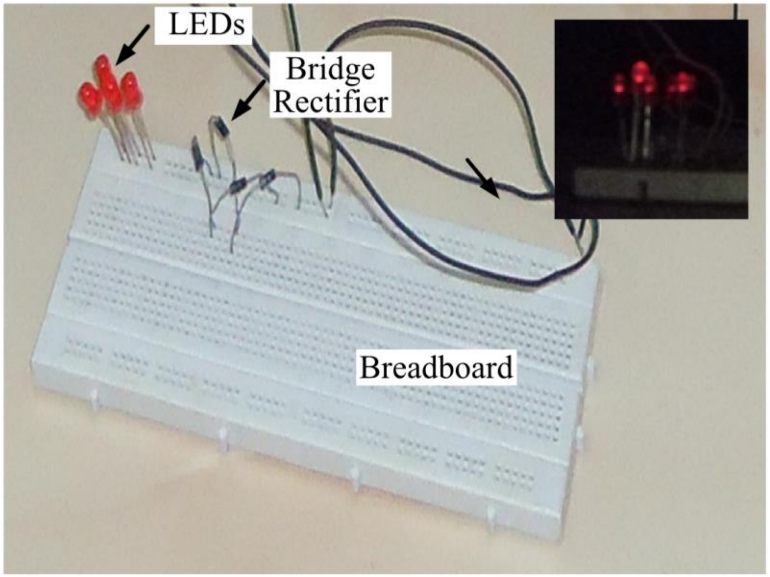


Fig: Experimental demonstration of light-emitting diodes powered through hybrid harvester.

The amount of power extracted from HH is adequate enough to power the wireless sensors and LEDs.

# Demonstration: Video

# Summary of the first part

- This study reports experimental and theoretical studies of a coupled piezo-electromagnetic hybrid energy harvester.
- Simplified analytical model provides a good approximation to the experimental results.
- Hybrid harvester operates over a broad range of frequencies, compared to the narrow operating frequency range in standalone devices.
- Simultaneous production of high current and the high voltage is obtained due to the coupling of piezoelectric and electromagnetic transduction techniques.
- Parameters are discussed with the perspective of optimizing the magnitude and bandwidth of the harvested power.

# II. Investigation of an array of electromagnetic energy harvester

# Electromagnetic energy harvester array

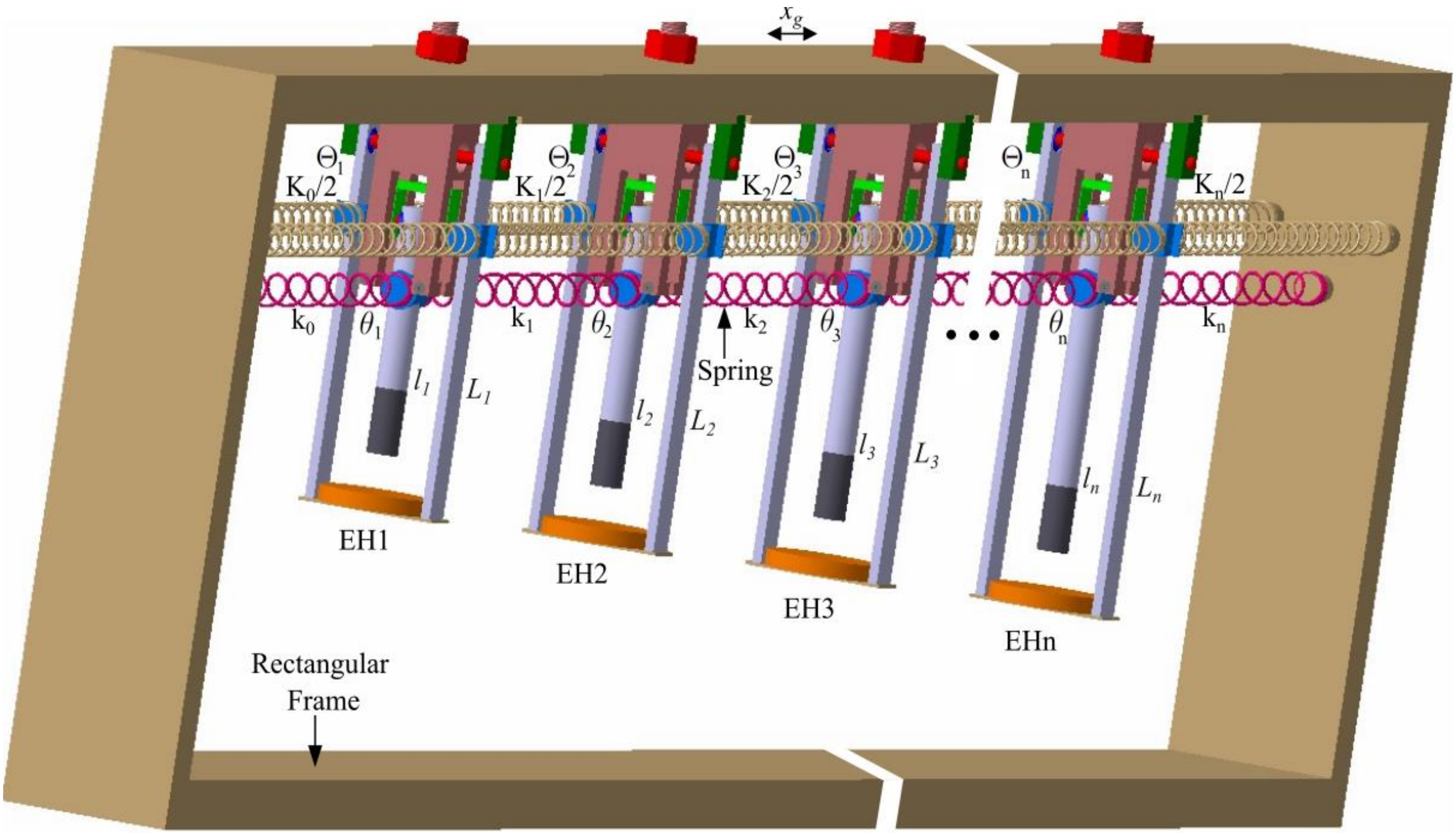


Physical Model

# Harvester Model : contd…

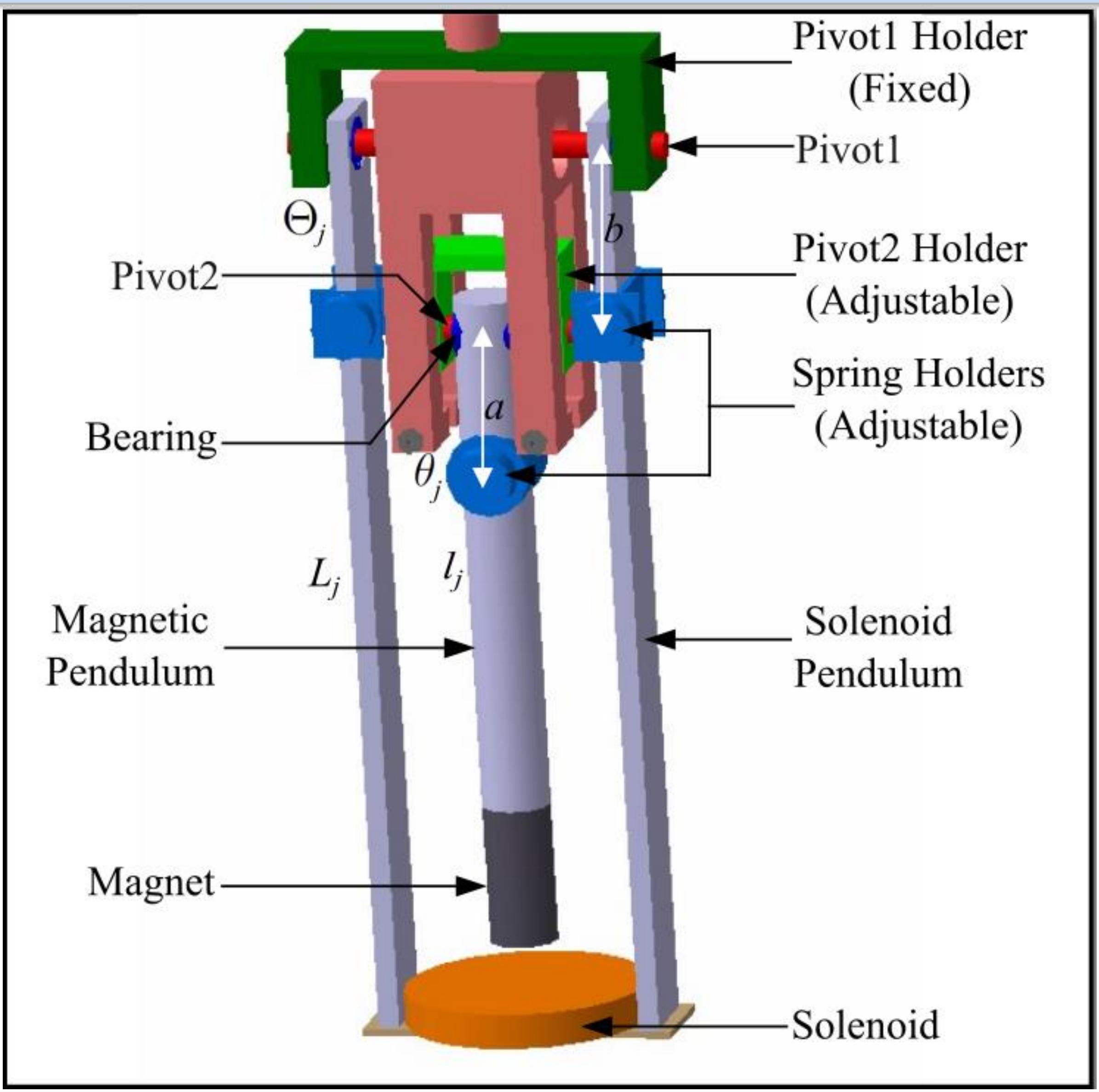


Closeup view

# Mathematical Model

Equations of motion of the $n$- pendulum array

$$m_j l_j^2 \ddot{\theta}_j(t) + c_j l_j^2 \dot{\theta}_j(t) + \bar{m}_j g l_j \sin\theta_j(t) + k_{j-1} a^2 [\sin\theta_j(t) - \sin\theta_{j-1}(t)] \cos\theta_j(t)$$
$$+k_j a^2 [\sin\theta_j(t) - \sin\theta_{j+1}(t)] \cos\theta_j(t) = -m_j l_j \ddot{x}_g(t) \cos\theta_j(t);$$
$$\{\ j{=}1,2,3\ldots n, \quad \theta_{j-1}(t) = 0;\ at\ j=1, \quad \theta_{j+1}(t) = 0;\ at\ j=n$$

$$M_j L_j^2 \ddot{\Theta}_j(t) + C_j L_j^2 \dot{\Theta}_j(t) + \bar{M}_j g L_j \sin\Theta_j(t) + K_{j-1} b^2 [\sin\Theta_j(t) - \sin\Theta_{j-1}(t)] \cos\Theta_j(t)$$
$$+K_j b^2 [\sin\Theta_j(t) - \sin\Theta_{j+1}(t)] \cos\Theta_j(t) = -M_j L_j \ddot{x}_g(t) \cos\Theta_j(t);$$
$$\{\ j{=}1,2,3\ldots n, \quad \Theta_{j-1}(t) = 0;\ at\ j=1, \quad \Theta_{j+1}(t) = 0;\ at\ j=n$$

Nondimensional form

$$\mu_j \alpha_j^2 \ddot{\theta}_j' + 2\zeta_j \mu_j \alpha_j^2 \Omega_j \dot{\theta}_j' + \bar{\mu}_j \alpha_j \sin\theta_j' + \beta_{j-1} [\sin\theta_j' - \sin\theta_{j-1}'] \cos\theta_j'$$
$$+\beta_j [\sin\theta_j' - \sin\theta_{j+1}'] \cos\theta_j' = \mu_j \alpha_j \Omega^2 \lambda \sin(\Omega\tau) \cos\theta_j';$$
$$\{\ \theta_{j-1}' = 0;\ at\ j=1, \quad \theta_{j+1}' = 0;\ at\ j=n$$

$$\hat{\mu}_j \hat{\alpha}_j^2 \ddot{\Theta}_j' + 2\hat{\zeta}_j \hat{\mu}_j \hat{\alpha}_j^2 \hat{\Omega}_j \dot{\Theta}_j' + \hat{\bar{\mu}}_j \hat{\alpha}_j \sin\Theta_j' + \hat{\beta}_{j-1} (\sin\Theta_j' - \sin\Theta_{j-1}') \cos\Theta_j'$$
$$+\hat{\beta}_j (\sin\Theta_j' - \sin\Theta_{j+1}') \cos\Theta_j' = \hat{\mu}_j \hat{\alpha}_j \Omega^2 \lambda \sin(\Omega\tau) \cos\Theta_j';$$
$$\{\ \Theta_{j-1}' = 0;\ at\ j=1, \quad \Theta_{j+1}' = 0;\ at\ j=n$$

# Mathematical Model : contd…

Nondimensional parameters :

$$\mu_j=\frac{m_j}{m_1};\ \hat{\mu}_j=\frac{M_j}{m_1};\ \bar{\mu}_j=\frac{\bar{m}_j}{\bar{m}_1};\ \hat{\bar{\mu}}_j=\frac{\bar{M}_j}{\bar{m}_1};\ \alpha_j=\frac{l_j}{l_1};\ \hat{\alpha}_j=\frac{L_j}{l_1};$$

$$\zeta_j=\frac{c_j}{2m_1\omega_1};\ \hat{\zeta}_j=\frac{C_j}{2m_1\omega_1};\ \beta_j=\frac{k_j a^2}{m_1 l_1^2\omega_1^2};\ \hat{\beta}_j=\frac{K_j b^2}{m_1 l_1^2\omega_1^2};\ \lambda=\frac{X_g}{l_1};\ \Omega=\frac{\omega}{\omega_1}$$

Total Power

$$|P_t| = \frac{1}{2}\sum_{j=1}^{4}\Omega^2\zeta_{emj}(\hat{\alpha}_j\Theta_j - \alpha_j\theta_j)^2$$

Table: List of harvester configurations with different coupling combinations

| | | | |
|---|---|---|---|
| SaMH | UC | | UC SaMH |
| | C&UG | | C&UG SaMH |
| | C&G | | CG SaMH |
| SaSH | UC | | UC SaSH |
| | C&UG | | C&UG SaSH |
| | C&G | | C&G SaSH |
| MSH | UC SH | UC MH | UC MSH |
| | | C&UG MH | UC SH with C&UG MH |
| | | CG MH | UC SH with C&G MH |
| | C&UG SH | UC MH | C&UG SH with UC MH |
| | | C&UG MH | C&UG MSH |
| | | CG MH | C&UG SH with C&G MH |
| | C&G SH | UC MH | C&G SH with UC MH |
| | | C&UG MH | C&G SH with C&UG MH |
| | | CG MH | C&G MSH |

Coupled and ungrounded (C&UG)

$$\beta_0, \beta_n, \hat{\beta}_0, \hat{\beta}_n = 0$$

Uncoupled and ungrounded (UC)

$$\beta_q, \hat{\beta}_q = 0$$

# Results:

Linear dynamics

$\lambda = 0.01$

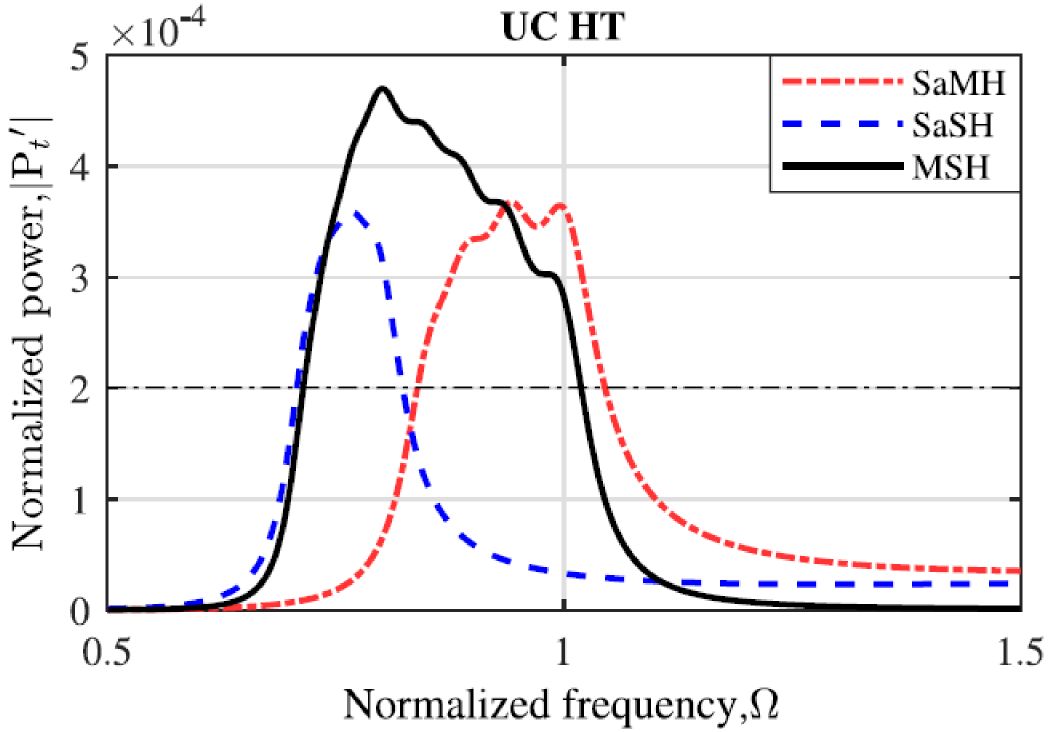


Power @ $2 \times 10^{-4}$, the bandwidth of the UC MSH increases by 45.57% compared to UC SaMH and by 162.07% compared to UC SaSH.

Figs : Frequency response of the uncoupled harvesters' normalized power [at $\lambda = 0.01$].

# Results: contd…

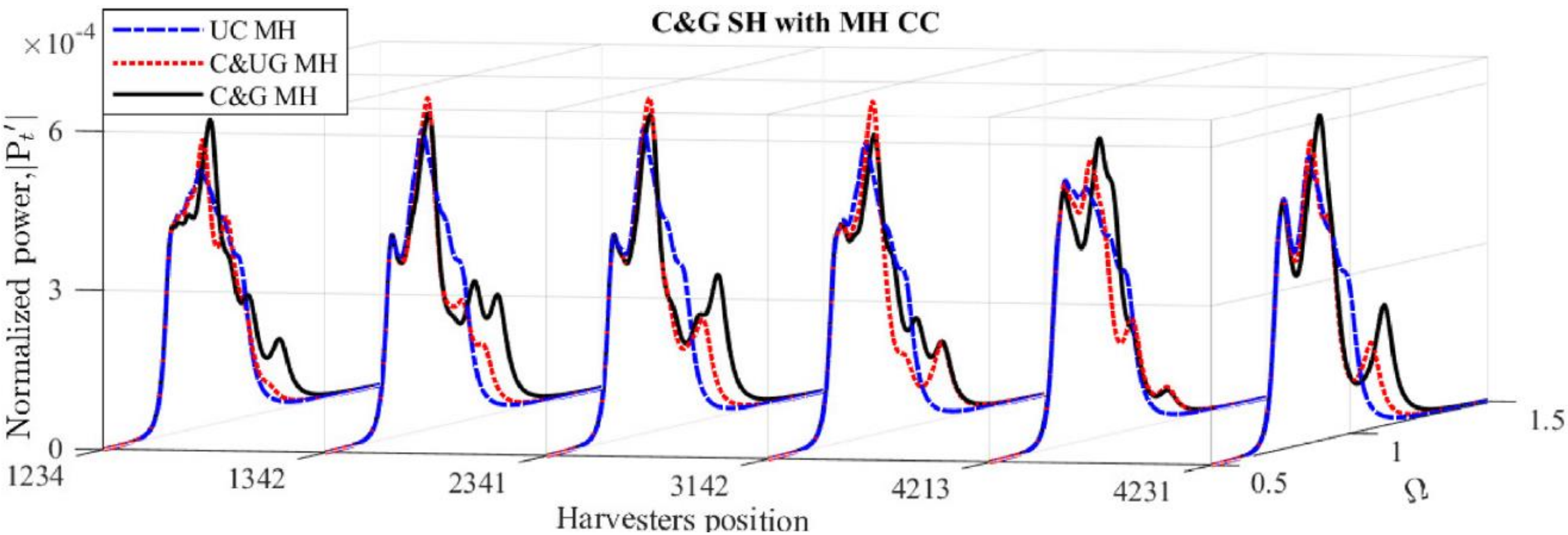


Figs : Comparisons of the total harvested normalized power of C&G SH with MH CC across various positions of the harvesters. [ Note: only six of them are shown for visual clarity]

> Each harvester in the harvesting array is designed to have a different resonant frequency, so their performance varies depending on their location when they are coupled.

Spring with equal stiffness → n!/2 possible combinations

| | | | | | | | | | | | |
|---|---|---|---|---|---|---|---|---|---|---|---|
| **1234** | **1423** | **1342** | **2314** | **2143** | **2341** | **3214** | **3142** | **3421** | **4213** | **4312** | **4231** |

# Results: contd…

Table : Comparisons of relative power density

| Coupling ↓ Combinations | | Harvesters Position→ | 1234 | 1423 | 1342 | 2314 | 2143 | 2341 | 3214 | 3142 | 3421 | 4213 | 4312 | 4231 |
|---|---|---|---|---|---|---|---|---|---|---|---|---|---|---|
| | | | Relative Power Density (%) | | | | | | | | | | | |
| MH | UC | | 100 | | | | | | | | | | | |
| MH | C&UG | | 100.31 | 101.33 | 100.87 | 101.56 | 101.16 | 101.08 | 101.19 | 101.77 | 100.52 | 100.99 | 100.74 | 100.92 |
| MH | C&G | | 109.84 | 111.82 | 112.75 | 108.87 | 109.36 | 112.97 | 107.10 | 110.00 | 110.96 | 106.89 | 108.02 | 110.47 |
| SH | UC | | 66.35 | | | | | | | | | | | |
| SH | C&UG | | 66.40 | 66.56 | 66.48 | 66.58 | 66.52 | 66.51 | 66.53 | 66.62 | 66.43 | 66.50 | 66.46 | 66.49 |
| SH | C&G | | 69.25 | 69.64 | 69.88 | 69.01 | 69.18 | 69.91 | 68.65 | 69.28 | 69.51 | 68.62 | 68.88 | 69.34 |
| MSH | UC SH | UC MH | 126.59 | | | | | | | | | | | |
| MSH | UC SH | C&UG MH | 126.37 | 126.34 | 126.25 | 126.57 | 126.47 | 126.17 | 126.30 | 126.62 | 126.27 | 126.38 | 126.52 | 126.51 |
| MSH | UC SH | C&G MH | 139.22 | 140.48 | 141.84 | 137.30 | 137.83 | 141.85 | 135.54 | 138.19 | 140.11 | 135.50 | 136.90 | 139.58 |
| MSH | C&UG SH | UC MH | 127.12 | 129.98 | 128.80 | 129.88 | 128.75 | 129.05 | 128.78 | 130.47 | 127.99 | 129.18 | 128.44 | 128.97 |
| MSH | C&UG SH | C&UG MH | 126.79 | 127.55 | 127.19 | 127.90 | 127.52 | 127.31 | 127.52 | 128.00 | 126.92 | 127.33 | 127.22 | 127.32 |
| MSH | C&UG SH | C&G MH | 139.63 | 141.88 | 143.15 | 138.09 | 138.76 | 143.38 | 136.03 | 139.42 | 140.93 | 135.87 | 137.30 | 140.32 |
| MSH | C&G SH | UC MH | 127.63 | 130.28 | 130.57 | 129.90 | 129.07 | 129.85 | 128.40 | 130.90 | 129.13 | 128.86 | 128.28 | 129.77 |
| MSH | C&G SH | C&UG MH | 127.02 | 127.35 | 127.05 | 127.99 | 127.61 | 127.05 | 127.61 | 128.00 | 127.04 | 127.47 | 127.39 | 127.40 |
| MSH | C&G SH | C&G MH | 140.86 | 142.96 | 144.44 | 139.05 | 139.80 | 144.59 | 136.82 | 140.41 | 142.21 | 136.65 | 138.27 | 141.47 |

$$RPD_H = \left(\frac{PD_H}{PD_{UCSaMH}}\right)100\ \%$$

$PD_H$ -power density of the respective harvester array.

$PD_{UCSaMH}$ -power density of the uncoupled MH array.

C&G SaMH, C&G SaSH, and C&G MH with SH CC in MSH give the maximum power density at the harvester position of 2341, and all other uncoupled/coupled combinations give the maximum power density at the harvester position of 3142.

# Experimental setup

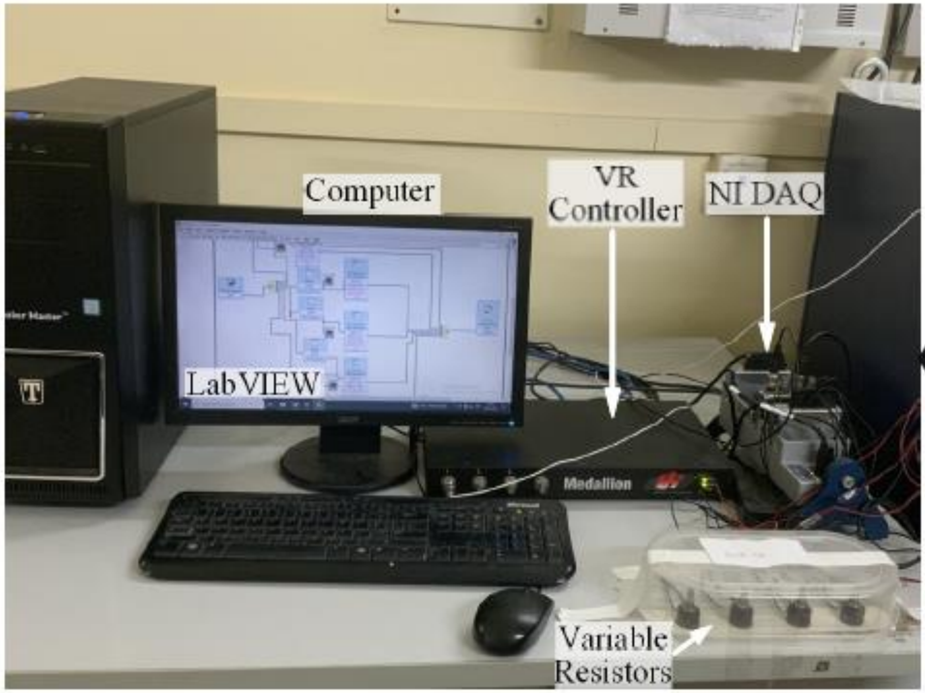


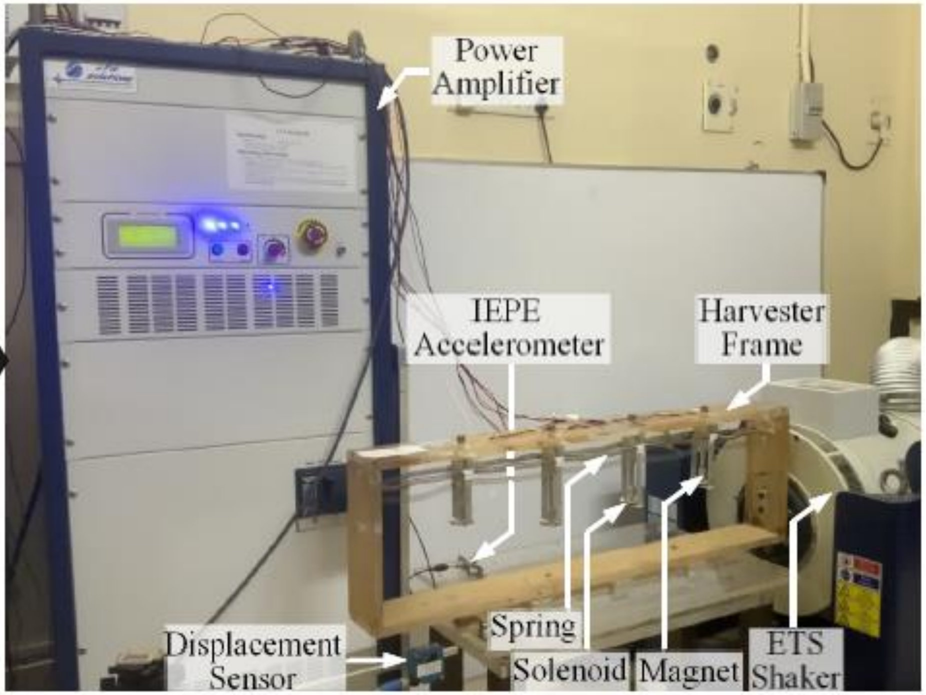


## Parameters and their values

| Description | Value | | | |
|---|---|---|---|---|
| Length of the MP, $l_j$ (mm) | 70 | 80 | 90 | 100 |
| Mass of the magnet part, $m_{m_j}$ (gm) | 17.6 | 17.6 | 17.6 | 17.6 |
| Mass of the MP rod, $m_{r_j}$ (gm) | 16.6 | 18.6 | 20.6 | 22.6 |
| Mechanical damping of the MP, $c_{me_j}$ (Ns/m) | 0.0064 | 0.0059 | 0.0056 | 0.0052 |
| Length of the SP, $L_j$ (mm) | 110 | 120 | 130 | 140 |
| Mass of the solenoid bobbin, $M_{s_j}$ (gm) | 17.2 | 17.2 | 17.2 | 17.2 |
| Mass of the SP strips, $M_{st_j}$ (gm) | 24.6 | 26.6 | 28.6 | 30.6 |
| Mechanical damping of the SP, $C_{me_j}$ (Ns/m) | 0.0071 | 0.0069 | 0.0066 | 0.0064 |

# Multiple electromagnetic hybrid harvester

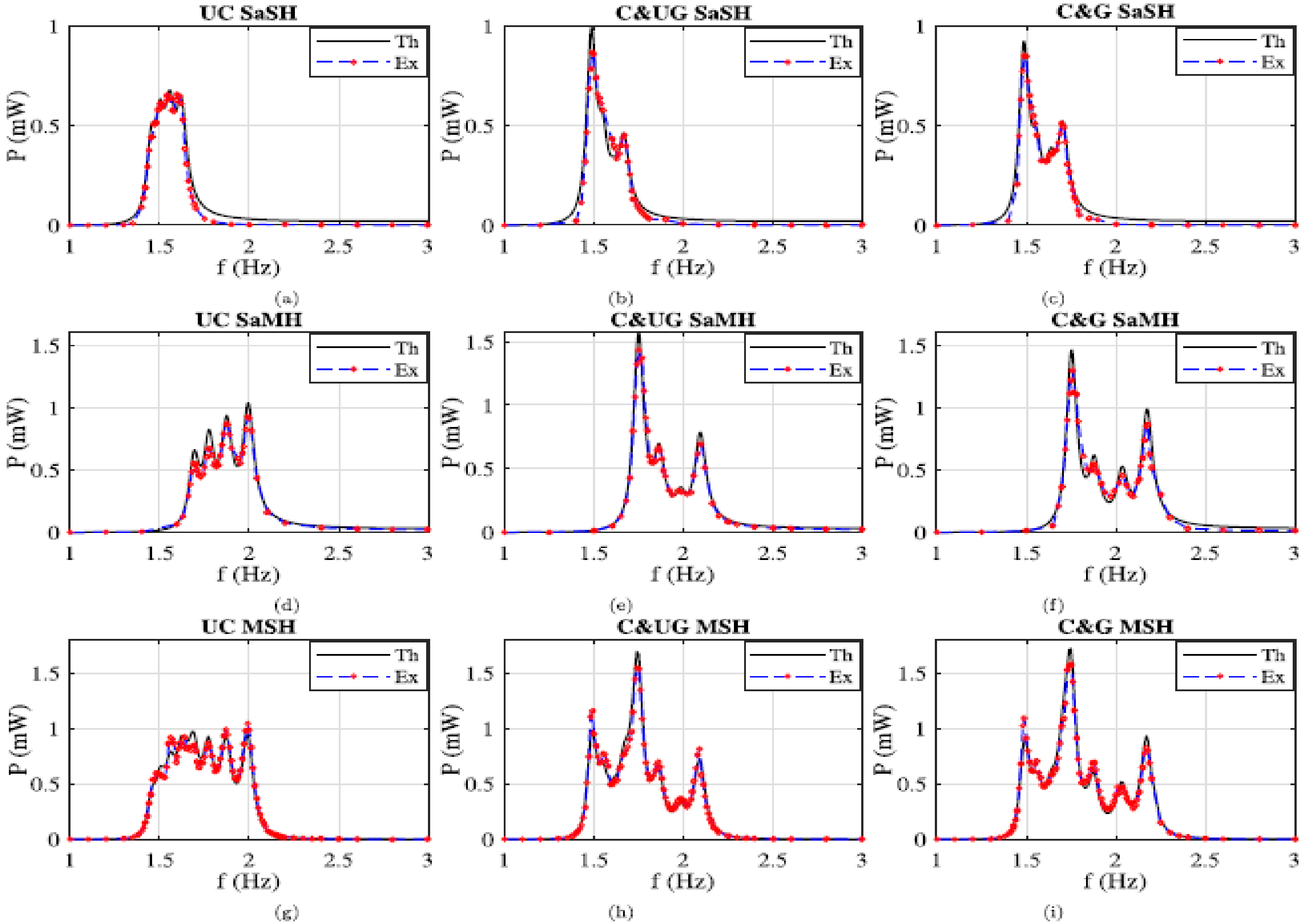


- Frequency sweep 1-3Hz
- Base excitation 0.7mm

Figs: Comparison of simulated and experimentally obtained powers for different types of harvesters with various coupling combinations.

# Conclusions

- This study reports a novel design of a pendulum-based array of electromagnetic vibration energy harvester.
- The investigations include three types of harvesters with different mechanical coupling configurations.
- The position of the harvesters was varied and analyzed.
- It is observed that, coupled and grounded magnetic-solenoid harvester gives the better performance.
- The experimental observations show good agreement with the theoretical results.

# Extended Research

1.Investigation of an array of pendulum-based electromagnetic nonlinear vibration energy harvester

Base excitation
3.5mm

2.Analysis of dual pendulum-based friction induced electromagnetic vibration energy harvester array

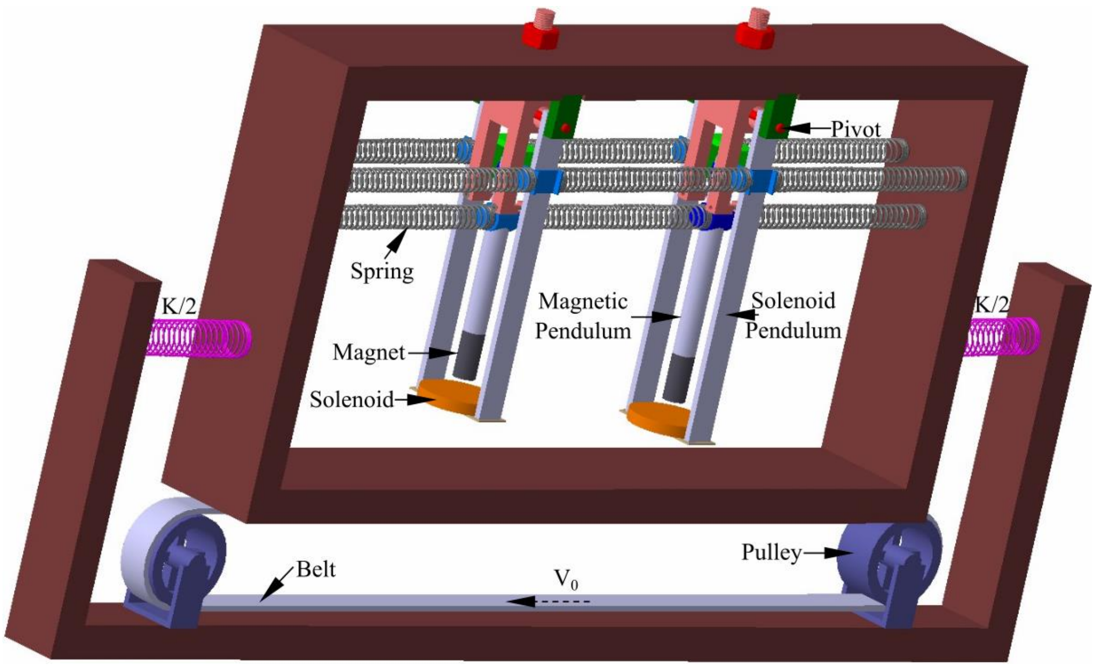


Stick-slip behavior
Stribeck model

# THANK YOU